Biaxial drawing of dried gels of ultra-high molecular weight polyethylene

Yoshihiro Sakai* and Keizo Miyasaka
Department of Organic and Polymeric Materials, Tokyo Institute of Technology, Ookayama, Meguro-ku, Tokyo 152, Japan
(Received 11 September 1987; revised 24 December 1987; accepted 8 January 1988)

The fine structure and properties of ultra-high molecular weight polyethylene (UHMW–PE) films prepared by simultaneous biaxial drawing of the dried gel at 135°C were studied as a function of draw ratio. Scanning electron microscopy showed that the drawn films comprise fibrils which are several tens of nanometres thick and endlessly long. The fibrils are not straight along their whole length but entangled with each other. This is the most important structural feature of biaxially drawn UHMW–PE film. The small angle X-ray scattering peak corresponding to the long spacing disappeared at a certain draw ratio ($\lambda = 10 \times 10$). The differential scanning calorimetry (d.s.c.) measurements indicated that extended chain type crystals increase with increasing draw ratio. The crystallinity estimated by density, d.s.c. and infrared absorption was much less than that of uniaxially drawn materials, although it slightly increased with increasing biaxial draw ratio.

(Keywords: ultra-high molecular weight polyethylene; gel film; simultaneous biaxial drawing)

INTRODUCTION

High modulus and high strength materials have been made of ultra-high molecular weight polyethylene (UHMW–PE) by various methods, such as a solution-crystallization technique referred to as the surface growth method[1-3] and a solution–gelation–drawing technique referred to as gel spinning/drawing[4-9], inclusive of dried gel film drawing[10]. The ultra-high drawability of UHMW–PE gels is considered to be due mainly to the appropriate number of chain entanglements well adjusted by dilution of polymer in the solvent and the following gelation. Structural studies on uniaxially drawn UHMW–PE materials revealed that their surprisingly high strength and modulus are due to the particular structure characterized by disappearance of the amorphous diffuse halo and the long spacing peak in wide and small angle X-ray scattering, respectively[11,12]. The long spacing corresponds to the crystalline and amorphous phases stacked in series.

Although studies on biaxial drawing of UHMW–PE and the structure and properties of biaxially drawn materials are important from both scientific and processing points of view, many fewer of these studies have been made than on uniaxially drawn materials. Sakami and coworkers[13] investigated the fine structure and morphology of UHMW–PE prepared by crystallization after being uniaxially and biaxially drawn in the molten state, by means of differential scanning calorimetry (d.s.c.), X-ray diffraction and scanning electron microscopy (SEM). They suggested that oriented fibrils containing extended chain crystals were produced in the specimens drawn biaxially and subsequently crystallized.

Kaito and coworkers[13] investigated the mode of crystal orientation and the effects of molecular weight on fine structure in UHMW–PE films prepared by biaxial drawing in the molten state and subsequent cooling. They showed that the crystallographic c-axis tends to lie on the film plane and that the biaxially drawn films with viscosity averaged molecular weight $M_v = 27 \times 10^5$ have a fibrous structure, while samples with $M_v = 7 \times 10^5$ have a lamellar structure. It should be remarked that both Sakami's and Kaito's studies were made for the usual bulk specimens but not for gel specimens.

Minami and coworkers[15] studied the mechanical properties of UHMW–PE films made by simultaneous or successive biaxial drawing of the gel films. Their attainable maximum draw ratio was $\lambda = 16 \times 16$, giving a tensile modulus of about 7 GPa.

We are interested in the maximum draw ratio in biaxial drawing of UHMW–PE gel films and the resulting fine structure of the highly biaxially drawn films. We have studied the extreme fine structure of uniaxially drawn UHMW–PE using single crystal mats[11,12], which were considered to be the most effective specimen for this sort of study. It is also interesting to elucidate the difference in the fine structures of uniaxially and biaxially drawn films. In uniaxial drawing, the fibrils, which are the most important structural elements in drawn materials, are almost linear and orient only in the direction of drawing. In biaxial drawing, however, the fibrils may not be linear throughout their full length, orienting in all directions on the film plane. This situation necessarily causes non-parallel contact between fibrils, resulting in some entanglement of fibrils. This fibrillar entanglement must itself affect (deteriorate) further drawability and the properties of the resultant films. It is expected that once a fibrillar entanglement is formed, disentanglement must be very difficult without breakage of one of the participant fibrils and that the final drawability must depend on the number of fibrillar entanglements.

In the work described in this Paper, simultaneous biaxial drawing of UHMW–PE films, prepared by a gelation method, was studied with particular attention paid to the structure and properties of the drawn films.

* Research fellow from KAO Corporation

0032-3861/88/091608-07$03.00

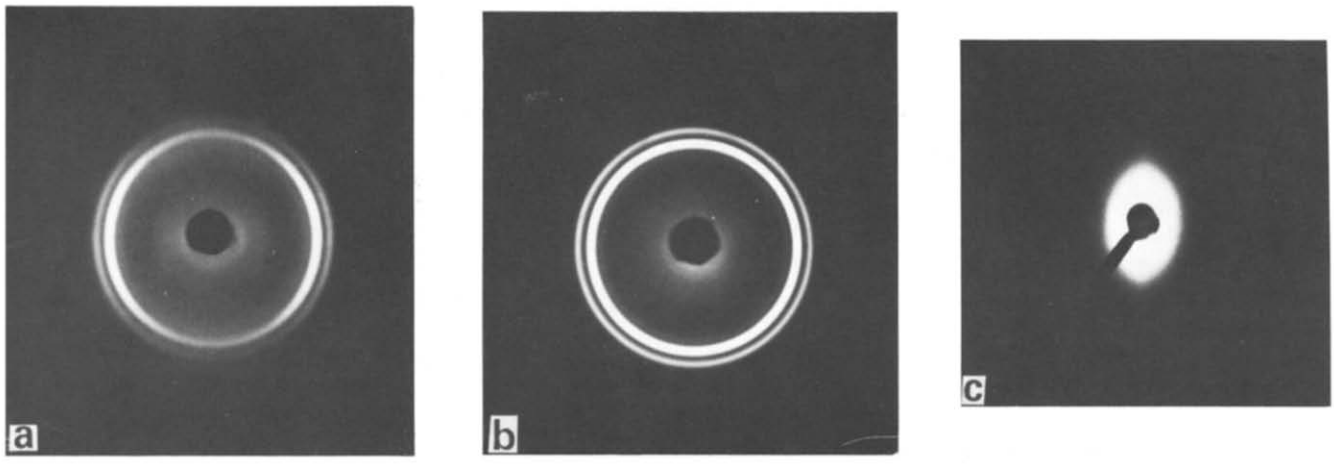

Figure 1 (a), (b) WAXD and (c) SAXS photographs of the original dried sheet. The incident beam is parallel to the sheet plane in (a) and (c), and normal in (b). The thickness direction is vertical in (a) and (c)

The results obtained are discussed in relation to previous data on uniaxially drawn materials.

EXPERIMENTAL

Sample preparation

In this work we used UHMW–PE Hizex Million (Mitsui Petrochemical Co. Ltd) with $M_v = 4.5 \times 10^6$. A homogenized decahydronaphthalene solution containing 4 wt% polymer was prepared in a separate flask at 160°C. The solution was stabilized by 0.5 wt% (based on the polymer) of an antioxidant di-tert-butyl-*p*-cresol. The solution was cooled gradually to room temperature to make the gel. The gel was taken out of the flask and pressed between aluminium boards under a pressure of 100 kg cm^{-2} at 150°C for 10 min, followed by quenching in water at 20°C. When the compression was carried out below 150°C, films of uniform thickness could not be obtained. The temperature of the compression machine was 150°C, and the temperature of the gel was difficult to estimate during the compression. Thus it is not certain what structural changes occurred during the compression. However, the fact that uniform films were obtained under this condition and that resultant films had the same mode of crystal orientation as that of single crystal mats or the usual dried gel films seems to imply that some partial melting of crystals might occur during compression. Subsequently, the gel sheet was dried at room temperature. The thickness of the dried gel sheets was 0.13–0.11 mm.

Figures 1a and *c* are, respectively, wide angle X-ray diffraction (WAXD) and small angle X-ray scattering (SAXS) photographs of the original dried film, both taken with the incident beam parallel to the sheet plane. The WAXD photograph (*Figure 1b*) taken with the beam normal to the sheet plane showed a uniform (isotropic) Debye ring pattern. These WAXD patterns indicate that the *c*-axes of crystals orient in the thickness direction of the sheet, although the degree of orientation is not high. The SAXS photograph has a meridional two-point pattern, indicating that the crystal interfaces orient parallel to the sheet plane. The long spacing estimated from the SAXS peak obtained using a position-sensitive proportional counter (PSPC) was 12 nm. These structural aspects are similar to those of single crystal mats of both medium molecular weight (MMW) PE[16] and UHMW PEs[11] and to those of dried gels[17,18] from solution. It is interesting to note that in contrast to the case described in this Paper the mats and dried gels were made without being heated at high temperature. Samples of 10×10 cm^2 were cut from the sheet for simultaneous biaxial drawing performed at 135°C using an Iwamoto biaxial film stretcher.

Characterization methods

WAXD photographs were taken by a flat camera with Ni-filtered Cu-Kα radiation from a Rigaku XG working at 35 kV and 40 mA. The WAXD intensity was measured using a scintillation counter with a pulse height analyser. SAXS photographs were taken by a vacuum camera with Ni-filtered Cu–Kα radiation from a Rigaku Rota Flex RU-200 working at 50 kV and 180 mA. Pinhole collimators 0.3–0.5 mm in diameter were used in SAXS measurements. The long spacing was evaluated from the SAXS intensity peak maximum obtained using a scintillation counter and a Rigaku 30C PSPC.

Infrared spectra to study the chain conformation were recorded using a Perkin–Elmer 1710 *FT*i.r. spectrometer. D.s.c. measurements to study the melting behaviour were made at a constant rate of heating of 10°C min^{-1}, using a Seiko Densi SSC/580 differential scanning calorimeter. The melting point and the heat of fusion were calibrated with indium (melting point 156.5°C, heat of fusion 28.8 J g^{-1}), as the standard material.

The density was measured using an ethanol–water density gradient column at 25°C. Dynamic mechanical properties were measured at 20°C using a Toyo Seiki Rheolograph Piezo at a frequency of 10 Hz. The scanning electron microscopic (SEM) observation was carried out for samples whose surfaces were coated with gold, using a JEOL JSM-350 SEM.

Estimation of crystallinity

Crystallinity was determined from infrared (i.r.) absorbance of gauche bands, heat of fusion and density. The i.r. crystallinity was calculated from the equation derived from two empirical relations obtained by Okada and Mandelkern[19]:

$$X = (58.1 - 0.19Y)/(5.92Y + 57.0)(1/1.02)$$

where Y is the ratio of absorbance at 1368 cm^{-1} to that at 1894 cm^{-1}, and the factor 1/1.02 is a correction factor to give $X = 1.0$ for $Y = 0$. In the calculation of d.s.c.

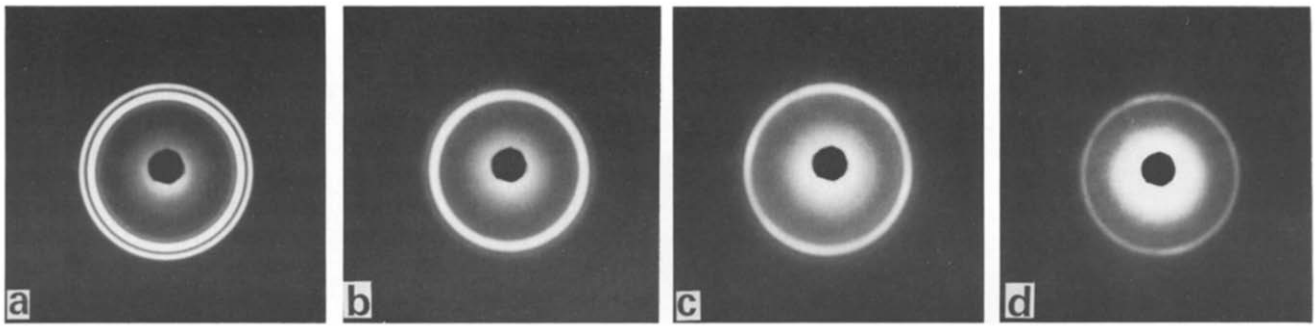

Figure 2 WAXD photographs, taken with the incident beam normal to the film plane, of simultaneously biaxially drawn UHMW–PE films for various biaxial draw ratios, λ: (a) 1 × 1; (b) 4 × 4; (c) 10 × 10; (d) 16 × 16

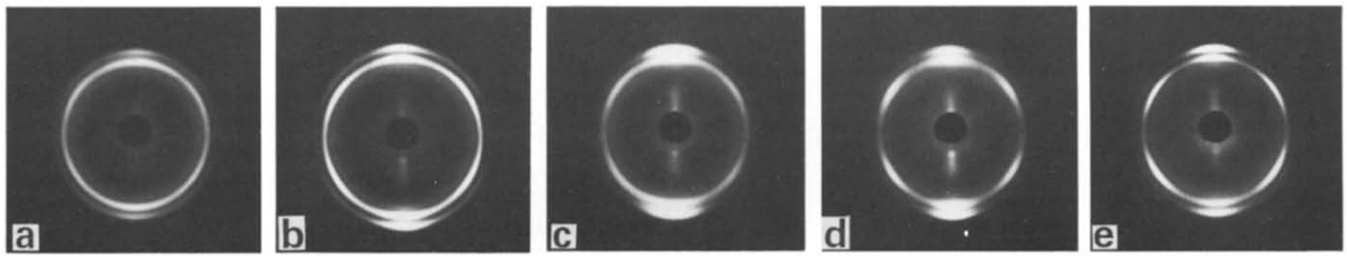

Figure 3 WAXD photographs, taken with the incident beam parallel to the film plane, of simultaneously biaxially drawn UHMW–PE films. The thickness direction is vertical. (a) $\lambda = 4 \times 4$; (b) 6 × 6; (c) 10 × 10; (d) 12 × 12; (e) 16 × 16

crystallinity, 293 J g^{-1} (reference 20) was used as the heat of fusion of PE crystal. The heat of fusion of samples was estimated from the total area under the melting thermogram, although the melting profile changed depending on draw ratio. In the calculation of crystallinity from the density, 1.00 (reference 21) and 0.855 g cm^{-3} (reference 22) were used as the density of the crystalline and amorphous phases, respectively.

RESULTS AND DISCUSSION

Figures 2 and *3* show WAXD photographs of simultaneously biaxially drawn UHMW–PE gel films, taken with the incident beams normal and parallel to the film plane, respectively. In *Figure 2* the diffraction pattern comprises rings with approximately uniform intensity along them, indicating that the films have a cylindrosymmetrical structure around the thickness direction, as expected from the mode of simultaneous biaxial drawing. *Figure 2* also shows that in highly drawn specimens the (200) diffraction ring has disappeared, while in the original specimen it appears with the second strongest intensity after the (110) diffraction ring. This result suggests that some modes of planar orientation of crystals are induced by biaxial drawing as well as orientation of the chain axes parallel to the film plane. The preferred crystal plane orientation is also induced in highly uniaxially drawn UHMW–PE film[23].

Figure 3 gives the information about crystal orientation more effectively than *Figure 2*. First, we can see that the WAXD pattern of drawn specimens is similar to that which would be obtained by a 90° rotation of the pattern of the original specimen (compare *Figure 3* with *Figure 1a*). This means that the chain axes of crystals changed their mode of orientation so as to lie randomly on the film plane. Second, we can see that the (110) diffraction intensity is concentrated into six spots on the Debye–Sherrer ring; two on the meridian, and four in the diagonal directions. On the other hand, the (200) diffraction spots appear with strong intensity on the meridian and with very weak intensity in the diagonal directions. These characteristic WAXD patterns indicate the coexistence of two modes of crystal plane orientation. The first is the mode in which the *a*-axis orients in the thickness direction of films. The meridional (200) and diagonal (110) spots come from this mode. The second is the mode in which the (110) plane orients parallel to the film plane, as suggested by the meridional (110) and weak diagonal (200) spots. These modes of crystal orientation are similar to those in rolled MMW–PE bulk films[24].

An important item of information given by *Figure 3* is that the degree of crystal orientation is not as high as that in uniaxially drawn specimens, as suggested by the width of the azimuthal intensity distribution of the (110) and (200) spots. Further, we can see that weak but sharp diffraction spots appear just inside the (110) diffraction on the meridian of highly drawn specimens in *Figure 3*. According to Seto *et al.*[25], the strong $(001)_{mono}$ diffraction spots of the monoclinic form of PE crystal appear at $2\theta = 19.5°$ for Cu–Kα. The chain axis is taken as the *b*-axis in Seto's lattice. Thus the diffraction spots on the meridian, appearing just inside the (110) diffraction, are identified as the $(001)_{mono}$ diffraction of the monoclinic form. It is interesting that the monoclinic form crystals are caused by high biaxial drawing at 135°C, for the form is known to be very unstable at high temperatures[25]. The monoclinic form was never caused in uniaxial drawing of UHMW–PE mats at 100°C[12].

Figure 4 shows WAXD intensity curves obtained with the incident beam normal to the film plane, corresponding to *Figure 2*. The decrease in the (200) intensity relative to the (110) intensity with increasing biaxial draw ratio is related to the preferred orientation of the (200) plane, as discussed in relation to *Figure 3*.

The (110) diffraction itself decreases in intensity with increasing draw ratio because of the plane orientation

discussed above. What should be noticed in *Figure 4* is the growth of a diffuse scattering appearing inside the (110) diffraction, with increasing biaxial draw ratio. This growth of a diffuse scattering must be related partly to the occurrence of the monoclinic form, as discussed for *Figure 3*. The broadness of the scattering peak, however, implies that it is difficult to assign the scattering only to the monoclinic crystalline diffraction, for in this region of scattering angle there are no monoclinic diffraction peaks other than the $(001)_{mono}$.

The amorphous scattering of PE usually appears with a very broad peak in this range of angles, and the crystallinity of the biaxially drawn films is not as high as that of uniaxially drawn UHMW–PE, the X-ray diffraction of which has no noticeable amorphous scattering. Thus it may be reasonable to consider that the diffuse scattering peak inside the (110) diffraction comprises the amorphous scattering as well as the $(001)_{mono}$ monoclinic diffraction. We should not, however, suppose that the fraction of the amorphous phase increases with biaxial drawing, for, as will be shown later, no evidence was obtained to show a decrease in crystallinity with increasing draw ratio. The amorphous scattering may change its profile when remarkable changes are caused in the mode or degree of orientation and in the packing state in the amorphous phase, even if the crystallinity remains unchanged. Thus we suppose that this growth of the broad peak appearing inside the (110) diffraction with increasing draw ratio is due mainly to these supposed structural changes in the amorphous phase, and partly to the increase in the amount of the monoclinic form.

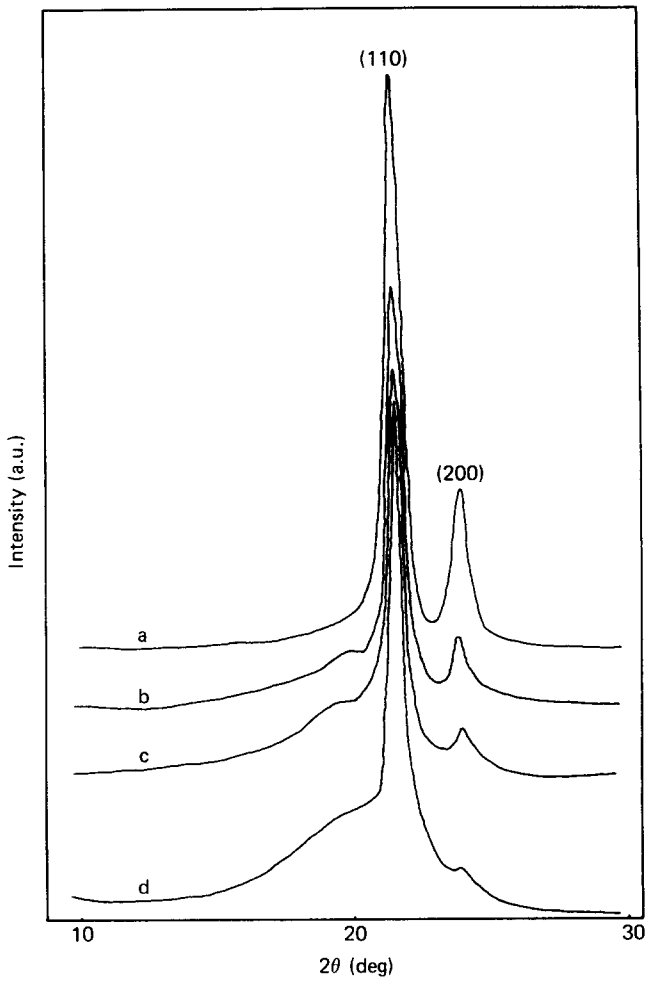

Figure 4 WAXD intensity curves of simultaneously biaxially drawn UHMW–PE films, taken with the incident beam normal to the film plane. (a) $\lambda = 1 \times 1$; (b) 4×4; (c) 10×10; (d) 16×16

Figure 5 shows SAXS photographs of biaxially drawn films taken with the incident beam parallel to the film plane. For biaxially drawn materials, an incident beam parallel to the film plane is more effective for structural study by SAXS than a beam normal to the film plane. This is because the former concentrates the fibrillar diffuse scattering on the meridian, and the peak intensity due to the long spacing on the equator. On the other hand, no such intensity concentration occurs with the beam normal to the film plane, and as a result two types of scattering appear in all directions, overlapping each other. As expected, the photograph of the (4×4) specimen is characterized by meridional diffuse scattering and equatorial two-point scattering. The former indicates that fibrils are formed by drawing, orienting their long axes parallel to the film plane. On the other hand, the latter indicates that each fibril has a structure related to the long spacing that is one of the most important structural aspects of crystalline flexible polymers. Further increase in the draw ratio accompanies the changes in the two types of SAXS scattering. The meridional fibrillar diffuse scattering increases the intensity, indicating the growth of the fibrillar structure. However, the equatorial two-point peaks gradually decrease in intensity with increasing draw ratio, and finally disappear completely in the samples drawn over (10×10). There are two possible reasons for the disappearance of the equatorial two-point peaks: the first is the disappearance of the long spacing in the fibrils, and the second is the large increase of long spacing beyond the resolution of the measurement. We suppose that the former may be the case, from analogy with the uniaxially drawn specimens.

Figure 6 shows the absorbance of three gauche bands

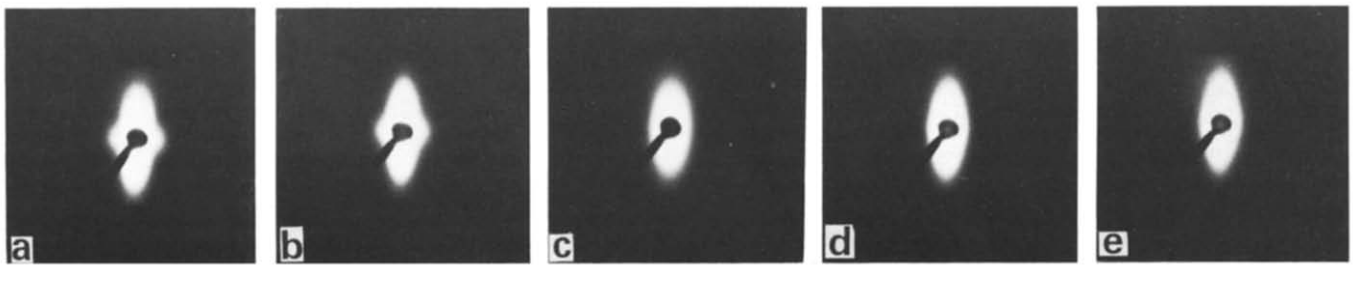

Figure 5 SAXS photographs, taken with the incident beam parallel to the film plane, of simultaneously biaxially drawn UHMW–PE films. The thickness direction is vertical. (a) $\lambda = 4 \times 4$; (b) 6×6; (c) 10×10; (d) 12×12; (e) 16×16

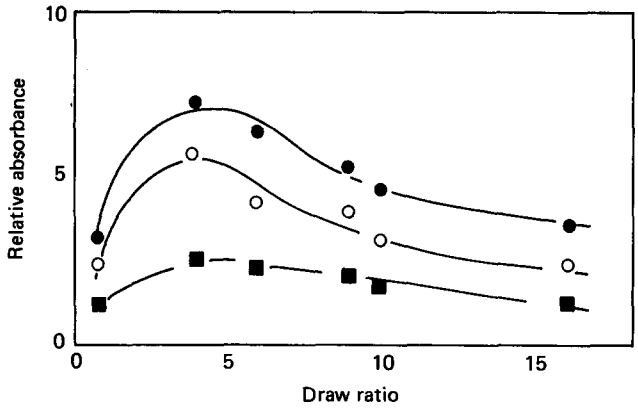

Figure 6 I.r. relative absorbance of gauche bands of simultaneously biaxially drawn UHMW–PE films as a function of biaxial draw ratio: ●, A_{1368}/A_{1894}; ○, A_{1352}/A_{1894}; ■, A_{1303}/A_{1894}

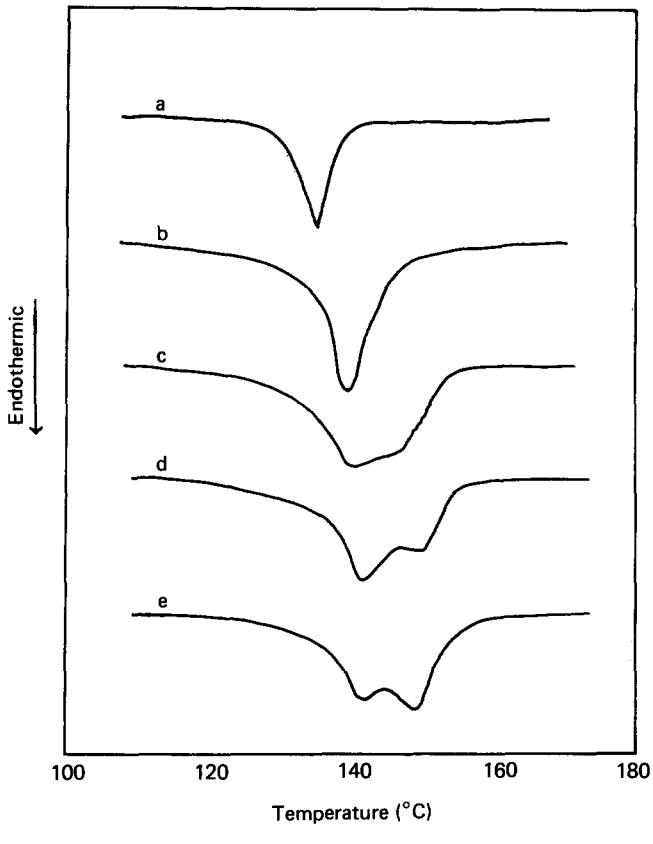

Figure 7 D.s.c. melting curves of simultaneously biaxially drawn UHMW–PE films: (a) $\lambda = 1 \times 1$; (b) 4×4; (c) 6×6; (d) 10×10; (e) 16×16

standardized with that of the crystalline 1894 cm^{-1} band as a function of biaxial draw ratio. These gauche bands have been assigned as follows[26]: 1368 cm^{-1} to GTTG or GTTG*, 1352 cm^{-1} to GG and 1303 cm^{-1} to GTG or GTG*. All the gauche bands have peaks in *Figure 6* at a draw ratio of (4×4). It is considered that the increase in the gauche fraction in the early stages of drawing is due to breakage of the lamellar structure, and that the subsequent decrease in the gauche fraction is due to extension of the amorphous chains and to chain unfolding on the crystal interfaces. It should be remarked that a substantial amount of gauche conformation still remains in the (16×16) specimen.

Figure 7 shows d.s.c. melting thermograms of biaxially drawn UHMW–PE films. For the (4×4) specimen no remarkable change appears in the profile, while the melting point shifts to higher temperatures compared with that of the original sample. For specimens with draw ratios over (6×6), the melting profiles become broader and consist of two peaks. The fraction of the higher temperature peak appearing at 150°C increases with increasing draw ratio, suggesting that the peak comes from the structure caused by high drawing. At the same time, this implies that even in the (16×16) specimen a comparatively large amount of crystals remains without being involved in the transformation into the highly drawn structure. Sakami *et al.*[13] assumed that a small amount of orthorhombic extended chain crystals having a melting point as high as about 150°C is produced by crystallization after biaxial drawing in the molten state. Their extended chain crystals may be similar to those corresponding to the fraction of high melting temperature in the thermograms of our specimens. The degrees of crystallinity of biaxially drawn films evaluated by density, i.r. and d.s.c. are shown in *Figure 8*, as a function of draw ratio. The values of crystallinity much depend on the method by which they were obtained, as is the usual case. The crystallinity increases very slightly with increasing draw ratio. However, the crystallinity is less than that of uniaxially drawn specimens, whose crystallinity is about 80% and 90% at $(\times 15)$ and $(\times 100)$[12], respectively, as averaged values of d.s.c., density, i.r. and X-ray crystallinity.

SEM photomicrographs of the biaxially drawn UHMW–PE films are shown in *Figure 9*. The (1×1) photograph (*Figure 9a*) shows that particles about 5 μm in diameter are the main structural units in the original dried gel sheets. According to *Figure 1*, a comparatively high degree of crystal orientation is caused in these particles. Because of the particle shape and the particular mode of crystal orientation these particles may be called two-dimensional spherulites. In the (1×1) photograph each particle seems to be connected with its neighbours, through many very thin short fibrils which are supposed to have been formed during preparation of the gel sheet. These thin fibrils connecting the particles must play an important role in the subsequent biaxial drawing.

In the (4×4) specimen, fibrillar structure appears with a comparatively large number of remaining particles (see *Figure 9b*). The most striking features in the photograph of the (4×4) specimen are that the fibrils have larger

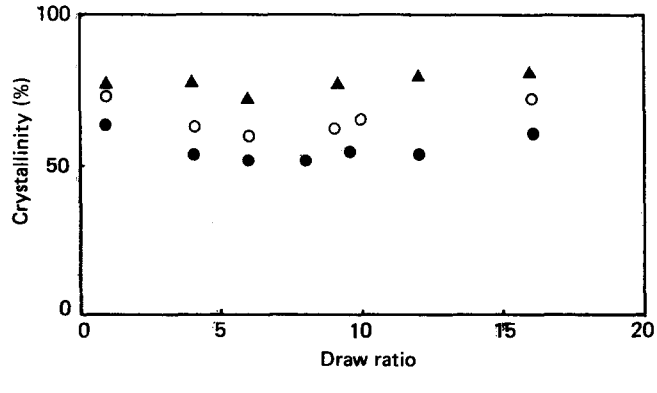

Figure 8 Crystallinity of simultaneously biaxially drawn UHMW–PE films as a function of biaxial draw ratio: ▲, from density; ○, from i.r. absorbance; ●, from heat of fusion

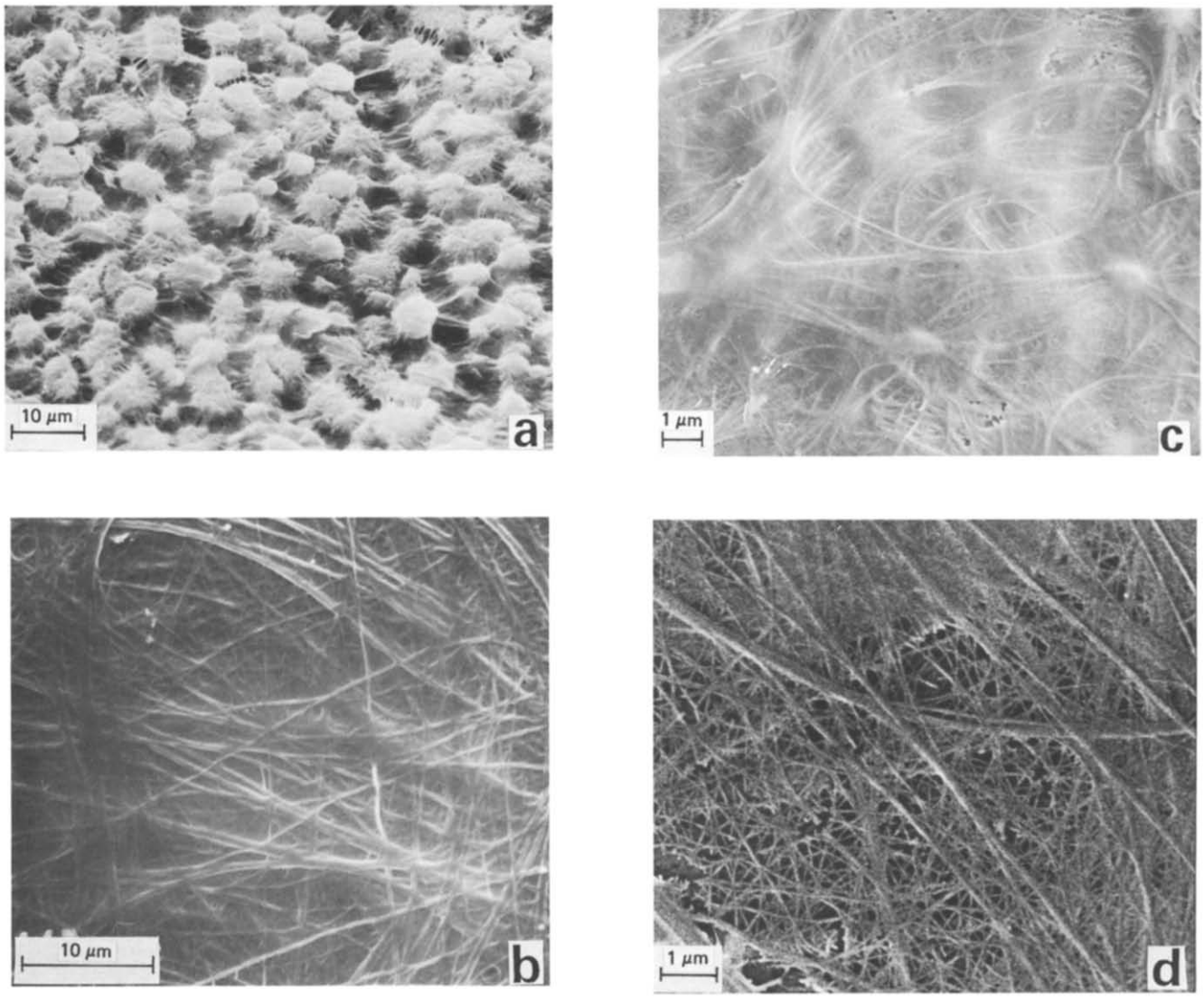

Figure 9 SEM photographs of simultaneously biaxially drawn UHMW–PE films: (a) $\lambda = 1 \times 1$; (b) 4×4; (c) 10×10; (d) 16×16

aspect ratios than expected from a draw ratio of (4×4) and that the fibrils are not straight but bent. We had supposed before the experiments that the fibrils might be linearly extended, orienting at random in all the directions, lying on the film plane. The particular features of the fibrils observed indicate that their origin is not due to simple plastic deformation of the original structure but due to a mixture of different mechanisms such as plastic deformation and a kind of melting induced by severe mechanical actions and the recrystallization under the particular circumstances. In uniaxial drawing these features of fibrils are difficult to detect, because all the fibrils are extended straight to align parallel to the direction of drawing.

In the (10×10) photograph (*Figure 9c*), the particle structure almost disappears, and the film comprises fibrils. In the (16×16) photograph (*Figure 9d*), microfibrils further increase in number, although some thick fibrils still remain without being split. The thickness of each microfibril is several tens of nanometres. It is interesting to note that the microfibrils form networks. We can see some characteristic places in the photograph which indicate a thick fibril being split into microfibrils. It seems that the fibrils are finer in the (16×16) photograph than in the (10×10) one. This implies that the fibrils become finer through thinning of fibrils themselves, as well as splitting of thick fibrils.

In the (16×16) photograph microfibrils form complicated networks with entanglements as the junction points; each fibril seems to have a junction point (entanglement) at about every 0.5 μm along its length. These networks of microfibrils must resist further drawing, because it is very difficult to disentangle the fibrils. Thus it should be considered that this type of fibrillar network is the final structure that we can reach by simultaneous biaxial drawing of UHMW–PE films.

An interesting question is whether the (16×16) specimen can be drawn further or not, so that the remaining thick fibrils may be transformed completely into microfibrils. We have not succeeded in further drawing over (16×16). If it was possible, further drawing would result in the breakdown of the microfibrils at the junction points (entanglements). One can already see this sort of breakage of microfibrils in the (16×16) photograph. This breakage which occurs at the entanglements, at the same time, indicates that the breaking strength of biaxially drawn UHMW–PE films is not only related to slippage between neighbouring microfibrils and to extensional breakage of the fibrils, but also to a particular mode of breakage of the fibrils at the

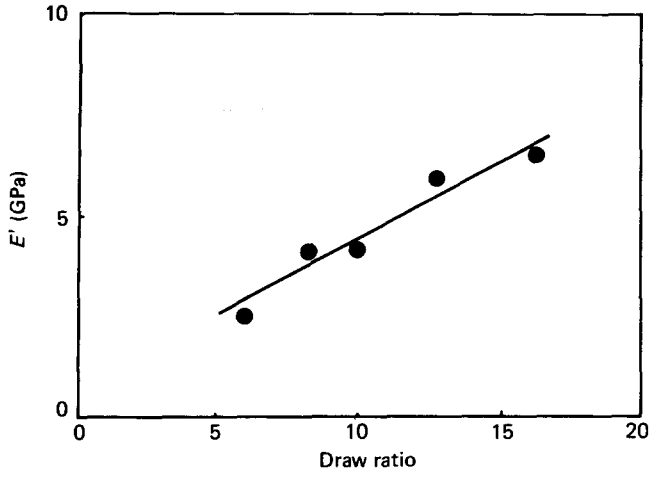

Figure 10 Storage dynamic modulus at 20°C of simultaneously biaxially drawn UHMW–PE films as a function of biaxial draw ratio

entanglement points. It is noteworthy that this mode of breakage of fibrils corresponds to a so-called 'knot strength', which is one of the most important modes of mechanical strength of fibrous materials, and that the 'knot strength' is always much smaller than the 'extensional strength'.

The dynamic mechanical storage modulus at 20°C of biaxially drawn UHMW–PE films is shown in *Figure 10* as a function of draw ratio. The modulus of the biaxially drawn films increased with increasing draw ratio. The largest attainable value of modulus was about 7 GPa, which is nearly the same as that achieved by Minami's group[15].

CONCLUSIONS

Dried gel sheets of UHMW–PE were drawn simultaneously biaxially, and the drawability, structure and properties of drawn films were studied with the following results. The highest draw ratio achieved to date is (16 × 16), and the dynamic storage modulus was 7 GPa. The drawn films comprised microfibrils several tens of nanometres thick which were not straight throughout their whole length but formed networks whose junction points are made of entanglements of the microfibrils. The SAXS peak corresponding to the long spacing disappeared at a draw ratio of (10 × 10), which suggests the disappearance of the structure composed of alternating crystalline and amorphous phases. D.s.c. indicated that the amount of extended chain crystals increased with increasing draw ratio. The crystallinity increased very slightly with increasing draw ratio. The value of the crystallinity, however, was much less than that in uniaxially drawn UHMW–PE.

REFERENCES

1 Zwijnenburg, A. and Pennings, A. *Colloid. Polym. Sci.* 1976, **254**, 868
2 Smook, J., Torfs, J. C., Hutten, P. F. and Pennings, A. J. *Polym. Bull.* 1980, **2**, 293
3 Barham, P. J. and Keller, A. *J. Mater. Sci.* 1980, **15**, 2229
4 Smith, P., Lemstra, P. J., Kalb, B. and Pennings, A. J. *Polym. Bull.* 1979, **1**, 733
5 Smith, P. and Lemstra, P. J. *Makromol. Chem.* 1979, **180**, 2983
6 Kalb, B. and Pennings, A. J. *J. Mater. Sci.* 1980, **15**, 2584
7 Kalb, B. and Pennings, A. J. *Polym. Commun.* 1980, **21**, 3
8 Smith, P. and Lemstra, P. J. *Polymer* 1980, **21**, 1341
9 Smith, P. and Lemstra, P. J. *J. Mater. Sci.* 1980, **15**, 505
10 Smith, P. and Lemstra, P. J. *Colloid. Polym. Sci.* 1980, **258**, 891
11 Furuhata, K., Yokokawa, T. and Miyasaka, K. *J. Polym. Sci., Polym. Phys. Edn* 1984, **22**, 133
12 Furuhata, K., Yokokawa, T. and Miyasaka, K. *J. Polym. Sci., Polym. Phys. Edn* 1986, **24**, 59
13 Sakami, H., Iida, S. and Sasaki, K. *Kobunshi Ronbunshu* 1977, **34**, 653
14 Kaito, A., Nakayama, K. and Kanetsuna, H. *J. Appl. Polym. Sci.* 1984, **29**, 2347
15 Minami, S. and Itoyama, K. *Am. Chem. Soc. Polym. Prepr.* 1985, **26**, 2, 245
16 Isikawa, K., Miyasaka, K. and Maeda, M. *J. Polym. Sci.* 1969, **A-2**, 7, 2029
17 Matsuo, M. and Manley, R. St. J. *Macromolecules* 1982, **15**, 985
18 Matsuo, M. and Manley, R. St. J. *Macromolecules* 1983, **16**, 1500
19 Okada, T. and Mandelkern, L. *J. Polym. Sci.* 1967, **A-2**, 5, 239
20 Cappaccio, G., Clements, J., Hine, P. J. and Ward, I. M. *J. Polym. Sci., Polym. Phys. Edn* 1981, **19**, 1435
21 Bunn, C. W. *Trans. Faraday Soc.* 1939, **35**, 482
22 Matsuoka, S. *J. Appl. Phys.* 1961, **32**, 2334
23 Smith, P., Lemstra, P. J., Pijpers, J. P. L. and Kiel, A. M. *Colloid Polym. Sci.* 1981, **259**, 1070
24 Frank, F. C., Keller, A. and O'Connor, A. *Phil. Mag.* 1958, **8**, 64
25 Seto, T., Hara, T. and Tanaka, K. *Jap. J. Appl. Phys.* 1968, **7**, 31
26 Wedgewood, A. R. and Seferis, J. C. *Pure Appl. Chem.* 1983, **55**, 873